[6]Lewis, J. E., Kubota, T., and Lees, L., "Experimental Investigation of Supersonic Laminar Two-dimensional Boundary-layer Separation in a Compression Corner with and without Cooling," *AIAA Journal*, Vol. 6, Jan. 1968, pp. 7-14.

[7]Holt, M. and Lu, T. A., "Supersonic Laminar Boundary Layer Separation in a Concave Corner," *Acta Astronautica*, Vol. 2, May-June 1975, pp. 409-429.

[8]Brown, S. N. and Stewartson, K., "Laminar Separation," *Annual Review of Fluid Mechanics*, Vol. 1, 1969, pp. 45-72.

[9]Hankey, W. L., "Prediction of Incipient Separation in Shock-wave/Boundary-layer Interactions," *AIAA Journal*, Vol. 5, Feb. 1967, pp. 355-356.

Direct Simulation Calculations of the Rarefied Flow Past a Forward-Facing Step

D. I. Pullin*
University of Melbourne, Parkville, Australia
and
J. K. Harvey†
Imperial College, London, England

Nomenclature

a_∞	= freestream speed of sound
ϵ	= molecular rotational energy
P_{fm}	= $\frac{1}{2}P_\infty(1+\sqrt{T_w/T_\infty})$; free molecular pressure for flat-plate flow
T	= translational temperature
T'	= 91.5 K; potential well temperature for Morse potential
T_x	= x component of T
T_R	= rotational temperature
T_w	= body temperature
u,v	= average gas velocity in x and y directions, respectively
V_x, V_y, V_z	= x, y, and z components of molecular velocity
λ_∞	= freestream mean free path

Introduction

THE development of the Direct Simulation Monte Carlo method[1] for the numerical simulation of the full nonlinear Boltzmann equation has made possible the calculation of rarefied transition flow about a variety of basic body shapes. Cases treated to date using this method include axisymmetric flow about spheres[2] and two-dimensional flow past cylinders[3] and the leading edge of flat plates[4-6] aligned with the freestream. Although much of this work has been for monatomic gases, schemes for the modeling of diatomic gases are now available, one of which has been applied to the flat plate[5,6] problem by the present authors.

In the present Note, we describe a detailed Direct Simulation calculation of the two-dimensional rarefied hypersonic flow of a diatomic gas past a forward-facing step placed $48\lambda_\infty$ downstream of a flat-plate leading edge. This basic departure from the flat-plate case is interesting, since it represents the interaction of a kinetic flow in the process of transition to a merged layer with a simple geometrical obstruction, leading to the possibility of step-induced flow separation.

Received June 10, 1976; revision received Oct. 19, 1976.
Index categories: Rarefied Flows; Supersonic and Hypersonic Flow.

*Lecturer, Dept. of Mechanical Engineering; formerly Research Assistant, Dept. of Aeronautics, Imperial College, London, England.
†Senior Lecturer, Dept. of Aeronautics. Member AIAA

The Direct Simulation method is a statistical technique in which the time evolution, including collisions, of a populous gasdynamic system is numerically simulated by following the simultaneous motion of a many orders-of-magnitude smaller number of sample particles. For a particular application, given a set of initial and boundary conditions together with a binary collision model the technique may be used to obtain statistical estimates of all desired flow properties including the distribution function, at any point in the gas. Accounts of the method and its relation to the Boltzmann equation may be found in Refs. 1 and 7.

Binary Collision Model

The binary collision model used in the present calculation is described in detail in Ref. 6. Briefly, the collision deflection angle and the Monte Carlo conditional collision probability[1] were treated using the spherical Morse potential.[8] For the treatment of the rotational-translation energy exchange in inelastic collisions with two internal degrees of freedom in rotation, a hybrid classical/statistical technique was employed. This method essentially combines a treatment of the inelastic exchange based on classical perturbation methods for a nonspherical potential[8] with a simple statistical relaxation technique.[7] The hybrid model is constructed so as to drive the gas into a state of local energy equipartition while retaining, for pair relative translational energy $\epsilon_t > 2kT'$, far from equilibrium, a detailed microscopic description of the exchange process. The model is efficient, requiring about 0.3 sec of CDC 7600 machine time per 1000 collision calculations. It correctly simulates rotational-translational temperature relaxation with the appropriate temperature dependence of the relaxation time,[8] and leads to approximate energy equipartition at equilibrium for temperatures up to 2000 K. At equilibrium, the velocity distribution is Maxwellian but due to overall violation of detailed balancing, the Boltzmann rotational energy distribution is not achieved.

Results and Discussion

The flow and body conditions, chosen to match those used in nitrogen experiments by Jeffrey[9] were $M_\infty = 22.9$, $T_\infty = 20$ K, $T_w/T_\infty = 14.4$. The freestream pressure and number density in these experiments were $P_\infty = 0.276$ N/m^2 and

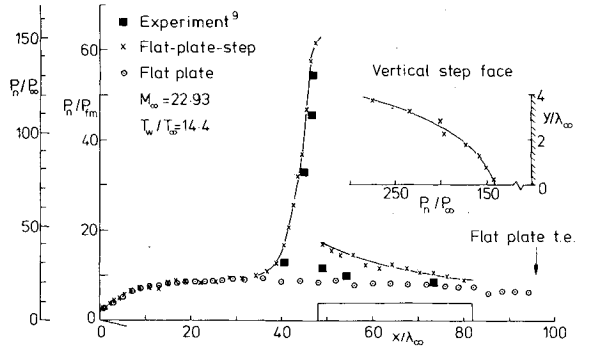

Fig. 1 Normal surface pressure.

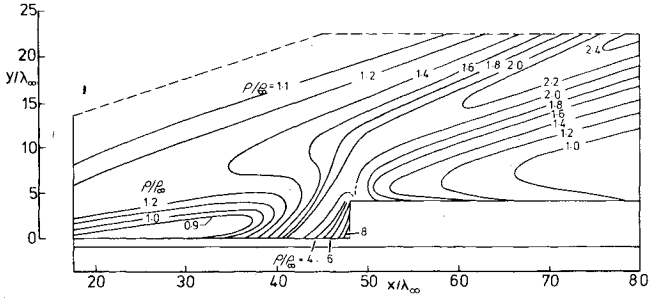

Fig. 2 Density contours $M = 22.9$, $T_w/T_\infty = 14.4$.

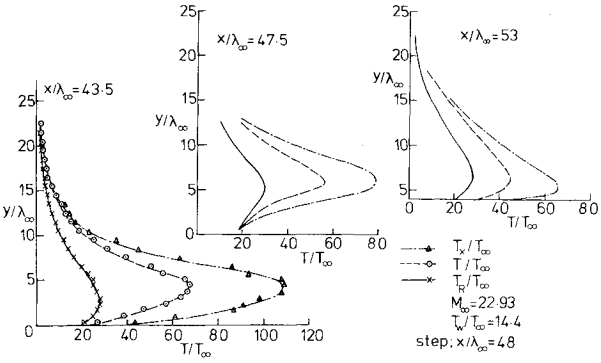

Fig. 3 Temperature profiles near step.

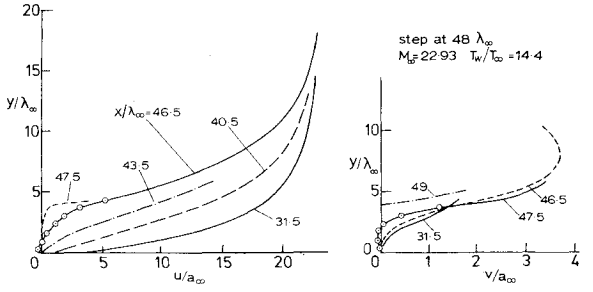

Fig. 4 Velocity profiles near step.

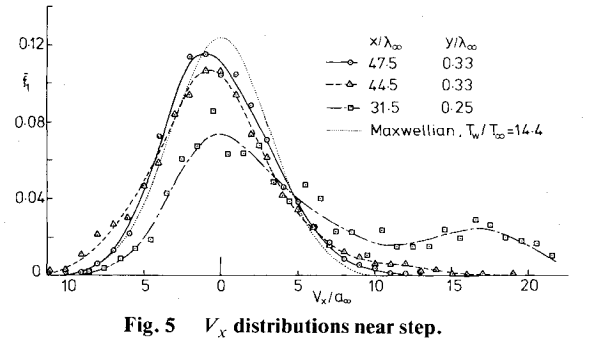

Fig. 5 V_x distributions near step.

$n_\infty \doteq 1.0 \times 10^{21}$ molecules/m^3, respectively. We take the definition of λ_∞ as

$$\lambda_\infty = 1/\sqrt{2}\pi\,\sigma^2 n_\infty \Omega^{(2,2)^*}(T_\infty/T')$$

where $\Omega^{(2,2)^*}$ is a collision integral from the transport theory,[10] and where for the Morse potential at $T_\infty = 20$ K we use the valae $\Omega^{(2,2)^*} = 2.115$. The molecule-surface law at the body boundary was taken to be fully diffuse with complete accommodation for both translational and rotational energy modes.

The particle sample size for estimation of flowfield and surface properties varied with the cell or surface segment dimensions, but was generally of the order 1000. Very near the step base, higher densities compensated for reduced cell sizes with resulting samples in the range 1000-3000.

Figure 1 indicates that the effect of the step on the plate normal pressure P_n is felt some 13-15λ_∞ upstream of the face. As the near surface flow undergoes rapid compression, P_n rises sharply in front of the step with no sign of a plateau. The normal pressure rises sharply up the vertical step face, the top of which is exposed to a high-speed stream and then drops by a factor of seven as the flow expands around the 90° top corner angle. Along the top horizontal surface P_n/P_∞ appears to approach the undisturbed flat plate pressure[5] also shown in Fig. 1. Forward of the step, quite good agreement is obtained with the uncorrected data of Jeffrey,[9] who measured pressure in blunt lipped cavities. For $x/\lambda_\infty > 48$ the near-surface flow is quite rarefied and corrections to the pressure data are necessary.

For $x/\lambda_\infty < 30$, the gas density (ρ/ρ_∞) contours shown in Fig. 2 are essentially those for an undisturbed flat-plate flow.[5] There then follows a fairly uniform compression of the flow in front of the step near the surface, whereas further out there is only a slight distortion of the developing merged layer shock. Downstream of the step, the contours recover their typical transition-merged layer shapes.

Temperature profiles shown in Fig. 3 indicate that much of the flow is in a highly nonequilibrium state. The partial profile at $x/\lambda_\infty = 47.5$ however, obtained in a column of cells of width $\Delta x = \lambda_\infty$ adjacent to the vertical step face, depicts the rapid approach to thermal equilibrium at T_w at the step base. By plotting flow quantities along the line $y/\lambda_\infty = -2/3\ x/\lambda_\infty + 32$ (which intersects the step base) it was inferred that at the very step base, the gas was in near equilibrium with $T/T_\infty = T_R/T_\infty = T_w/T_\infty \simeq 14.4$, $\rho/\rho_\infty \simeq 10$, $P_n/P_\infty \simeq 145$. Some $5\lambda_\infty$ downstream of the step the profiles begin to exhibit flat-plate characteristics once again with a large temperature jump at the surface.

The rapid x-wise deceleration of the flow near the step is illustrated in the u/a_∞ profiles shown in Fig. 4. Slip at the wall has vanished for $x/\lambda_\infty \gtrsim 43.5$ and for the $x/\lambda_\infty = 46.5$ profile there is evidence of reverse flow for $y/\lambda_\infty \lesssim 1$. Similarly, v/a_∞ is negative for $y/\lambda_\infty \lesssim 2$ in the normal velocity profiles in Fig. 4, thus indicating the presence of a region of clockwise circulating flow in a small, roughly triangular region with sides $\delta x \simeq 2\lambda_\infty, \delta y \simeq 3\lambda_\infty$ at the step base. On this scale, the local cell size ($\Delta x = \lambda_\infty, \Delta y = 2\lambda_\infty/3$) is rather coarse, and more detailed calculations would be required to probe the separation region. Note that $\lambda_{wall}/\lambda_\infty \simeq 1/10$ near the step base.

Histogram estimates of the reduced V_x distribution function $\bar{f}_1$ (integrated over V_y, V_z and ϵ coordinates) obtained in three near-surface cells upstream of the step are shown in Fig. 5. At the most upstream station, where the effect of the step has not yet been felt, $\bar{f}_1$ is bimodal with the small peak near $V_x/a_\infty = 17$ due to the collision products in the initial flat-plate flow. Further downstream $\bar{f}_1$ assumes a Navier-Stokes-like form as the now-continuum-flow rapidly approaches near equilibrium at T_w.

Conclusion

The calculations indicate that for the present configuration, the foward-facing step leads to a fairly localized disturbance to the overall flow, which further downstream reverts to the basic flat-plate merged layer structure. Along the plate near the step, however, the flow suffers a rapid deceleration and compression accompanying sudden transition to a near continuum Navier-Stokes-type state nearly in equilibrium at the body temperature. A very small region of separated and apparently circulating flow was detected very near the step base but the cell resolution was rather too coarse to examine it in detail. This effect might well be magnified by choosing a larger step height to plate forebody length ratio than has been treated herein.

Acknowledgment

This work was supported by the United Kingdom Science Research Council under Contract number B/RG 4313.

References

[1] Bird, G.A., "Direct Simulation of the Boltzmann Equation," *The Physics of Fluids*, Vol. 13, Nov. 1970, pp. 2676-2681.

[2] Bird, G.A., "Aerodynamic Properties of Some Simple Bodies in the Hypersonic Transition Regime," *AIAA Journal*, Vol. 4, Jan. 1966, pp. 55-60.

[3] Crawford, D.R. and Vogenitz, F.W. "Monte Carlo Calculations of the Shock Layer Structure on Adiabatic Cylinders in Rarefied Supersonic Flow," *Rarefied Gas Dynamics*, Ninth Symposium, Vol. 1, Ed. Becker, Fiebig, Dfvlr-Press, Potz-Wahn, 1974, Paper B.24.

[4]Vogenitz, F.W., Broadwell, J.E., and Bird, G.A., "Leading Edge Flow by the Monte-Carlo Direct Simulation Technique," AIAA Paper 69-141, New York, N.Y. 1969.
[5]Pullin, D.I., Harvey, J.K., and Bienkowski, G.K., "Hypersonic Leading Edge Flow of a Diatomic Gas by the Direct Simulation Method," *Rarefied Gas Dynamics*, Ninth Symposium, Vol. 1, Ed. Becker, Fiebig, Dfvlr-Press, Potz-Wahn, 1974, Paper D.5.
[6]Pullin, D.I. and Harvey, J.K., "A Numercial Simulation of the Rarefied Hypersonic Flat Plate Problem," Imperial College, London, England, Aero. Rept. 75-08, Sept. 1975.
[7]Borgnakke, C. and Larsen, P.S., "Statistical Collision Model for Monte-Carlo Simulation of Polyatomic Gas," Dept. of Fluid Mechanics, Technical University of Denmark, Lynby, Denmark, AFM 73-08; also AFM 75-02, 1975.
[8]Parker, J.G., "Rotational and Vibrational Relaxation in Diatomic Gases," *The Physics of Fluids*, Vol. 2, July 1959, pp. 449-462.
[9]Jeffrey, R.W., Dept. of Aeronautics, Imperial College, London, England, private communication, 1973.
[10]Hirschfelder, J.O., Curtiss, C.F., and Bird, R.B., *Molecular Theory of Gases and Liquids*, John Wiley & Sons Inc., New York, 1954, p. 527.

Oscillatory Burning of High-Pressure Exponent Double-Base Propellants

N. Kubota* and J. Kimura†
Japan Defense Agency, Tokyo, Japan

Nomenclature

a = coefficient in Vieilles burning rate law
C_d = nozzle discharge coefficient
K_n = ratio of propellant burning area to nozzle throat area
L^* = characteristic chamber length
n = pressure exponent in Vieilles burning rate law
p = pressure
p_c = mean chamber pressure
R = gas constant
r = linear burning rate
T_0 = propellant conditioning temperature
T_f = flame temperature
t = time
α = exponential growth constant of oscillation
α_t = thermal diffusivity of propellant
ρ_p = propellant density
τ = lead time of burning rate oscillation relative to pressure oscillation
τ_{ch} = chamber time constant, L^*/C_dRT_f
τ_{th} = thermal wave relaxation time, α_t/r^2
ϕ = amplitude of pressure oscillation
ω = frequency

Introduction

THE most familiar examples of low-frequency oscillatory burning are associated with chuffing experienced with double-base propellants at low pressures. Many of the experimental studies of chuffing and low-frequency burning have been conducted, and theoretical models have been presented to describe the burning behavior.[1-3] The models have been moderately successful; however, they use uncertain values for parameters such as the burning surface temperature and the activation energy of the burning surface.

In this Note, very-low-frequency burning of high-pressure exponent propellants is investigated using a strand burner and an L^* burner. The oscillatory burning was observed at intermediate pressures and was found to be different from the oscillatory burning of chuffing. The domain of the oscillatory burning (L^* vs p) is parabolic. An analytic model predicting the domain of oscillatory burning and the characteristics of oscillation in the case of very-low-frequency burning are presented.

Experiments

The propellant used in this study was a double-base propellant (51.0% nitrocellulose, 35.5% nitroglycerine, 12.0% diethyl phthalate, and 1.5% lead salicylate). The burning rate measurements were carried out with a nitrogen-pressurized chimney-type strand burner. Tests for unstable burning domains were done with a small end-burning-type rocket motor (L^* burner). Propellant grains were 114 mm diam × 40 mm long with the side and one end of the grain coated by an inhibitor. The burning pressure was measured by a strain-guage type pressure transducer mounted to the motor and was recorded by a visicorder. Since the chamber free volume increased with regressing the burning surface of the propellant grain, the L^* increased with burning time. The burning tests were conducted with $L^* = 4$-20 m.

The burning rate and pressure exponent of the propellant are largely dependent on pressure range. The burning rate characteristics are divided into four pressure zones, as designated in Fig. 1. The pressure exponent is 0.44 in zone I above 37 atm, approximately 1.1 in zone II between 37 and 21 atm, 0.77 in zone III between 21 and 11 atm, and 1.4 in zone IV below 11 atm.

The burning test results by the L^* burner showed that the burning behavior was very dependent on the pressure range and L^*. Typical pressure-time records are shown in Fig. 2. In zone I pressures above 37 atm, the burning was very stable, and neither oscillatory burning nor irregular burning was observed. In zone II where the pressure exponent was approximately unity, a sinusoidal oscillatory burning was observed when L^* was short. However, the oscillation diminished as L^* increased during burning. L^* observed oscillatory burning ranged 4-10 m, and the highest amplitude of pressure oscillation was approximately 7 atm. The frequency increased with increasing pressure from 6 Hz at 21 atm to 8

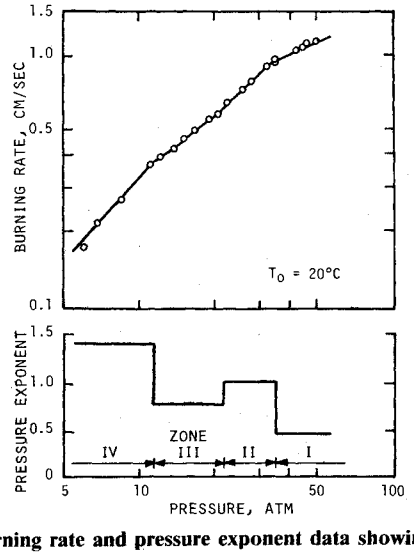

Fig. 1 Burning rate and pressure exponent data showing two high-pressure exponent zones.

Presented as Paper 76-668 at the AIAA/SAE 12th Propulsion Conference, Palo Alto, Calif., July 26-29, 1976; submitted Aug 16, 1976; revision received Oct. 22, 1976.
Index category: Combustion Stability, Ignition, and Detonation.
*Senior Research Fellow, Rocket Propulsion Lab. Third Research Center, Research and Development Institute, Member AIAA.
†Research Engineer, Rocket Propulsion Lab. Third Research Center, Research and Development Institute.